LACUNARITY AS A MEASURE OF TEXTURE*

Monika Krasowska†, Przemysław Borys
and Zbigniew J. Grzywna

Department of Physical Chemistry and Technology of Polymers
Section of Physics and Applied Mathematics, Silesian University of Technology
Ks. M. Strzody 9, 44-100 Gliwice, Poland

(Received January 12, 2004; revised version received March 15, 2004)

Lacunarity can work as a supplement for describing texture of self-similar objects. We propose a systematic study of this measure based on a set of carefully designed prototype structures, providing also a comparision to already existing measures (generalized fractal dimension). We also illustrate its applications to material science (describing changes in polymer surface during gold dispersion) and cellular biology (describing stains in cancer cells from two cell lines in two conditions). To measure lacunarity the gliding box method was used.

PACS numbers: 61.43. Hr

1. Introduction

"Texture is an elusive notion which mathematicians and scientists tend to avoid because they cannot grasp it. Engineers and artists cannot avoid it, but mostly fail to handle it to their satisfaction". This definition of texture descends from Mandelbrot's book [1] and is still valid. An important goal in many branches of science and especially in material science, biology and medicine is the quantitative analysis of the texture (patterns) of different objects. These patterns may often be complex, exhibit scale-dependent changes in structure, and may be difficult to quantify. Some progress in this direction has been made by means of fractal generalized dimension. It provides an acceptable good quantization of the structure and morphology of a wide range of different objects [2]. One can find examples of using fractal analysis for description of the microscopy output in different branches of

* Presented at the XVI Marian Smoluchowski Symposium on Statistical Physics, Zakopane, Poland, September 6–11, 2003.

† e-mail: krasowsk@zeus.polsl.gliwice.pl

science and technology: surface science (structure and morphology of materials surface) [3], porous materials [4], cellular biology (shape of cells) [5], *etc.* Very often however, it is not enough especially for sets with almost the same fractal dimension having quite different outlook otherwise. To make a progress, some new concepts are required.

One of such concepts is lacunarity. It was invented long time ago by Mandelbort [1] for measuring gaps in the texture. The name comes from Latin, *i.e.* lacuna stands for lack, gap, or hole. Unfortunately, this measure was until now very poorly examined, and it is difficult to tell, which features of the texture does it grasp best. In this paper we try to face this question by examining various, carefully constructed prototype structures of known differences, and noticing the changes in lacunarity. This enables one to learn, when application of this measure does make sense, and when this is not the case. We also compare it to the generalized fractal dimension, and show, that the areas of texture discrimination for those two measures are in many cases complementary.

In our paper we also investigate some previously proposed relations between fractal dimension and lacunarity, *i.e.* the linear relation between them [4]. We show that this relation is not always met, and we try to explain, why.

2. Lacunarity and its features

Various objects can exhibit different textures but still have the same fractal dimensions [1]. This problem in many cases can be avoided by using generalized fractal dimension (which usualy discriminates such textures), but sometimes even that is not enough. In such cases further progress can be achieved with help of lacunarity. Our studies show, that for textures with the same D_q (generalized fractal dimension, discussed in details previously in [2]) lacunarity can discriminate them very well (Fig. 1 and 2). From analysis of these images we can conclude about sensitivity of this measure to the shape of examined objects. This sensitivity is however limited by the resolution of image, and gliding box size (see difference for images koch2 and koch3).

Other studies show, that the lacunarity is a convenient measure of heterogeneity [6,7]. Low lacunarity indicates the homogeneity and translational invariance due to similar gap sizes, whereas high lacunarity indicates heterogeneity a wide range of gap sizes of a texture in question.

We measure lacunarity by the gliding box method. In this method the set under study is put on an underlying lattice with mesh size equal to $2a$; where a is less or equal to particle radius ε [6]. We consider a box of radius s which glides on this lattice. The gliding box is initially placed at upper left

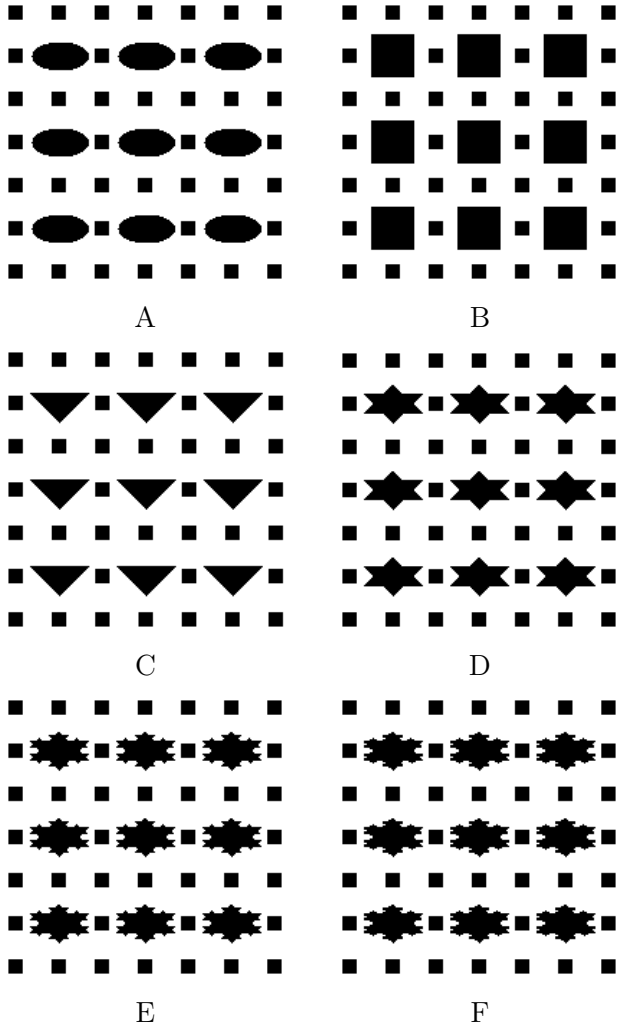

Fig. 1. Six prototype structures (A — ellipse, B — bars, C — koch0, D — koch1, E — koch2, F — koch3) with the same generalized fractal dimension D_q and different value of lacunarity Λ (see Fig. 2 for details). These structures have the same surrounding elements (small bars), and different cores of similar size.

corner of the image, and the number of light pixels in the image contained in the gliding box is counted to n_1. The box glides then over the entire image, moving to all N positions at which it covers at least one pixel of the image, at each location recording the number of light pixels (empty space) n_i in the box. The sequence of n_i values for $i = 1, 2, ..., N$ defines a probability distribution $Q_n(M, s)$ which represents the probability that a gliding box of

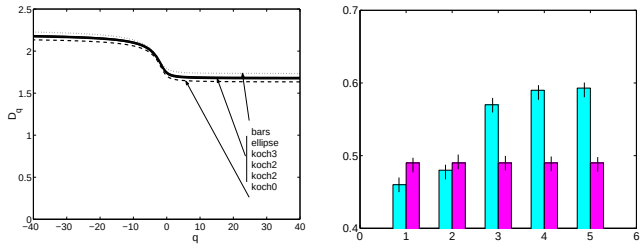

Fig. 2. Analysis of lacunarity and D_q spectrum for structures from Fig. 1: A — D_q (for ellipse, koch3, koch2, koch1, the plot overlaps). B — Λ (lightgray bars) and $\Delta D_q = D_{-\infty} - D_{\infty}$ (darkgray bars).

size s contains M light pixels. Lacunarity is defined in terms of moments

$$Z_{Q_n}^{(q)}(s) = \sum_{M=1}^{s^2} M^q Q_n(M,s) \tag{1}$$

of distribution $Q_n(M,s)$ by the ratio $\lambda(s)$

$$\lambda(s) = \frac{Z_{Q_n}^{(2)}(s)}{\left[Z_{Q_n}^{(1)}(s)\right]^2} = \frac{E(s^2)}{(Es)^2} = \frac{D^2 s}{(Es)^2} + 1 = \Lambda(s) + 1\,, \tag{2}$$

where Es stands for expected value, and $D^2 s$ for the variance. (Note, that lacunarity λ, as usually defined (*cf.* [8]), is always greater than one, but in some papers we meet lacunarities (Λ) lower than one, declared to be λ [9].)

Lacunarity is a function of three factors. First, of the size of gliding box. When this size increases, then also the average mass of the box gets bigger (which causes greater denominator in (2)). Simultanously, the probability that box masses will differ, decreases (because local features become averaged). Thus variance drops down, and similarly the numerator of (2).

Second variable in considerations is the fraction of map occupied P (as the mean number of occupied sites goes to zero, lacunarity goes to infinity — because of denominator in (2)); thus, sparser maps have higher lacunarities than dense maps. The final factor is the geometry of map (for a given P, higher lacunarity represents higher contagion) [7, 8].

Analysis, in this paper, has been performed on a PC computer using the public domain ImageJ program (developed at the U.S. National Institute of Health and available on the Internet at `http://rsb.info.nih.gov/nih-image/`). This program calculates an average Λ over a branch of gliding box sizes. Such analysis is in most cases good enough, but occasionaly (like

for cancer cell staining) when it is important to calculate the lacunarity of individual frame sizes, or lacunarity of a non-rectangular region, it needs extension. For such purposes we have written our own program.

In Fig. 3 we show the self-similarity range of lacunarity. As can be seen the lacunarity changes with the box size s. At large box sizes the lacunarity decreases, because all features of image become averaged into a kind of "noise". At small scales we are limited by the image resolution. There is however still quite a wide range of s in which the concept makes sense [6]. From this scaling behaviour we see, that choosing a proper gliding box size is an important problem. One way of dealing with this is to average the lacunarity over the whole range of scales, and check, the variance. If it is small, then we have just a small uncertainty about the calculated value of Λ. This is the case in the above mentioned program.

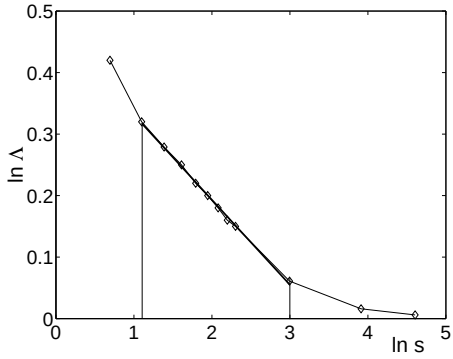

Fig. 3. Lacunarity Λ *versus* gliding box sizes (s) (in ln–ln coordinates) for structure F from Table IV.

3. Lacunarity versus fractality

When introducing the new physical measure the natural question arises how does it correspond to already existed ones. The simplest property of an object (set) is its average density. We can easily obtain a value for the density of material in search area by dividing the mass of tiles in the area by magnitude of search area [10]. Thus we have:

$$\sigma = \frac{nM}{L^2}\,, \tag{3}$$

where σ is the average density of the lattice area, L length of lattice, n number of tiles of mass M. Apart from density, there was a need to define

some quantity, which would measure the holes of the image. In a book of Kaye [10], who studied random walk generated lattices, there is a relation between "local density", lacunarity, and the fractal dimension D_0:

$$\frac{nM}{L^2} \sim \Lambda D_0 \,. \tag{4}$$

This gives a hint, that there should be a negative correlation between Λ and D_0.

Later reports try to investigate and complete the relationship between fractal dimension and lacunarity. Smith [9] observed negative correlation between fractal dimension and lacunarity based on analysis of neuronal cells. In Pomonis [4] paper, one can find another example of, essentially experimental relationship, between fractal dimension D_0 and lacunarity Λ

$$D_0 = 2.47 - 1.4\Lambda \,. \tag{5}$$

(Though a thermodynamic formalism, staying behind the lacunarity concept has not been proposed so far, there are several proposals concerning the fractal dimension, referring to $f(\alpha)$– formalism, known as multifractality, and related concepts, mostly toward quantification of possibly chaotic character of microstractures under examination, see [11] and Refs. therein.)

We obtain quite similar results for morphology of polymer surface (Fig. 4A) and structure of stains in cancer cells (Fig. 4B). (We realise, that in Fig. 4A there is only 6 values plotted due to the technical limitations of the technique used, but neverthless, it is worth mentioning as illustration of another process, which seems to exhibit expected behaviour). In contrary, for the set of prototype structures we obtain a plot which does not look linear at first sight. But when take a closer look, it appears to contain several clusters of linearly aligned values. These clusters correspond to similar prototype structures (Fig. 5 and Table I). From these results, we can speculate, that the linear relation applies only to surfaces, generated by similar mechanism, and consequently, where the images show similar type of regularity. So, when we don't observe negative correlation, it may happen, that in the examined process there are several surface generation mechanisms of different nature. This is partially seen in the prototype structures of P2 set (see Table I) where the dominating structure changes at some point from squares to circles. This is due to the fact, that we have here two mechanisms: change in radius of circles and opposite in direction, change in diameter of squares. These two mechanisms are however of similar nature, and correlation does not disrupt totally.

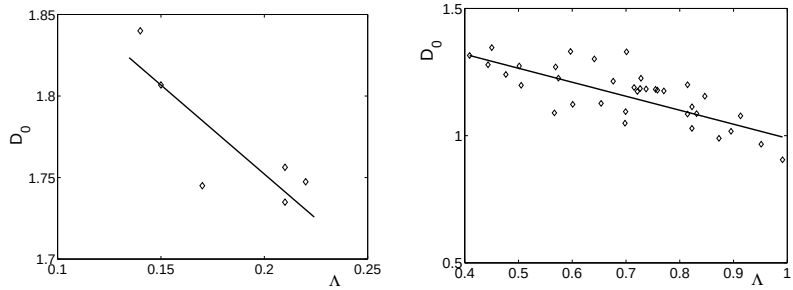

A B

Fig. 4. Fractal dimension (D_0) *versus* lacunarity (Λ) of two examples. A — Morphology of polymer surface during gold dispersion. $D_0 = 1.95 - 0.95\Lambda$ Correlation coefficient equal to 0.68. B — Structure of stain in cancer cells. $D_0 = 1.34 - 0.55\Lambda$ Correlation coefficient equal to 0.57.

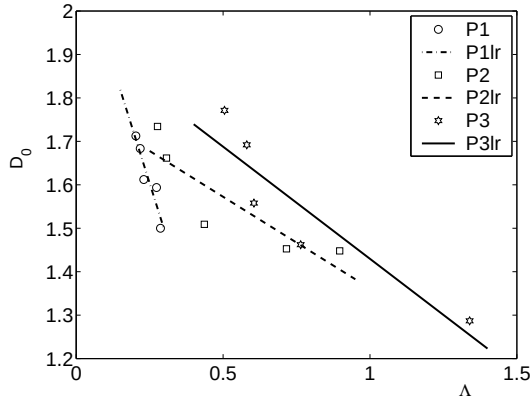

Fig. 5. Fractal dimension D_0 *versus* lacunarity Λ for different prototype structures (see Table I and III). For P1: $D_0 = 2.14 - 2.15\Lambda$ Correlation coefficient equal to 0.87. For P2: $D_0 = 1.78 - 0.42\Lambda$ Correlation coefficient equal to 0.77. For P3: $D_0 = 1.94 - 0.52\Lambda$ Correlation coefficient equal to 0.83.

Besides of the above considerations for fractal dimension, we can also see a relation of lacunarity to generalized fractal dimension. In figure 6 there is a comparision of these two measures for image set P2. We see, that lacunarity behaves complementary to generalized fractal dimensions, *i.e.* when the differences in fractal dimension are low, the differences in lacunarity get higher, and *vice versa*.

TABLE I

Prototype structures. P1: a carpet with uniformly distributed frames of various size. P2: a carpet with growing circles and decreasing squares. P3: dendrite tree based structure with differing number of branches (only nodes are plotted).

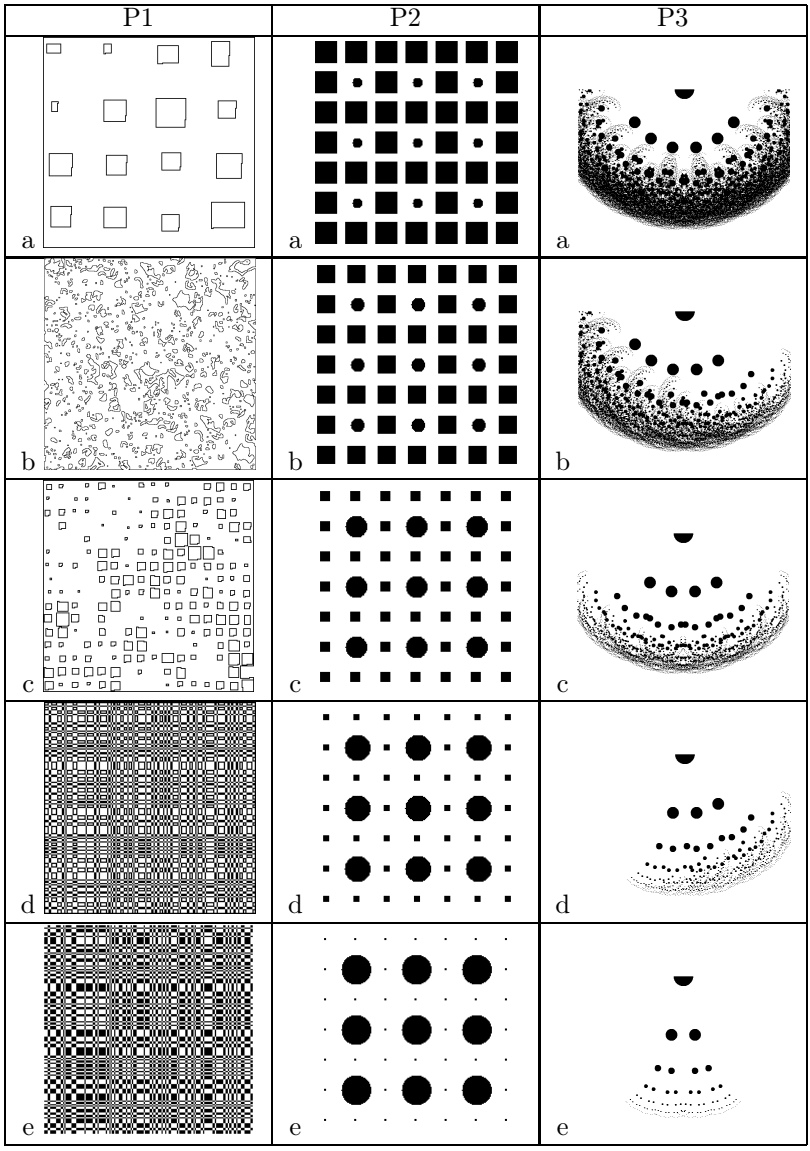

TABLE II

Lacunarity Λ and fractal dimension D_0 for prototype structures from Table I.

Name	Λ	D_0
P1a	0.20 ± 0.01	1.71 ± 0.01
P1b	0.22 ± 0.01	1.68 ± 0.01
P1c	0.23 ± 0.01	1.61 ± 0.01
P1d	0.27 ± 0.01	1.59 ± 0.01
P1e	0.29 ± 0.01	1.50 ± 0.01
P2a	0.28 ± 0.01	1.73 ± 0.01
P2b	0.31 ± 0.01	1.66 ± 0.01
P2c	0.44 ± 0.01	1.51 ± 0.01
P2d	0.72 ± 0.01	1.45 ± 0.01
P2e	0.89 ± 0.01	1.44 ± 0.01
P3a	0.50 ± 0.01	1.77 ± 0.01
P3b	0.58 ± 0.01	1.69 ± 0.01
P3c	0.60 ± 0.01	1.56 ± 0.01
P3d	0.76 ± 0.01	1.46 ± 0.01
P3e	1.33 ± 0.01	1.29 ± 0.01

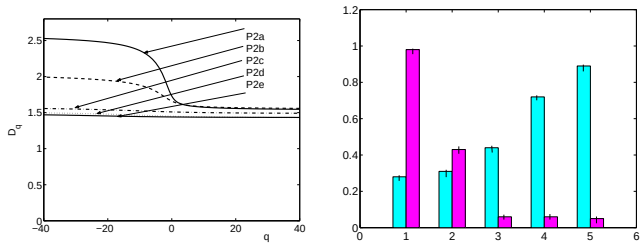

A B

Fig. 6. Analysis of lacunarity and D_q spectrum for structures P2 from Table I: A — D_q. B — Λ (lightgray bars) and $\Delta D_q = D_{-\infty} - D_{\infty}$ (darkgray bars).

4. Results and discussion

Aside of studying the prototype stuctures, we present the usage of lacunarity for two real-life cases: characterizing the polymer surface during gold dispersion and staining in cancer cells. (They are examples of two entirely different problems, for which we have the data available, having nothing in common.)

The problem of gold clusters embedding in crystallizing bisphenol A polycarbonate, treated as diffusion with drift in time changing medium was presented previously [12]. In this presentation fractal analysis had been

used to describe differences in polycarbon membrane surface morphology during the gold dispersion. We describe surfaces of two kinds of membranes (thickness: 2 μm and 3.5 μm) after 10h, 24h, 35.5h and 96.5h gold dispersion (Table III).

TABLE III

Structure and morphology of polymer surface during gold dispersion.

Time [h]	Thickness 2μm	Thickness 3.5μm
10		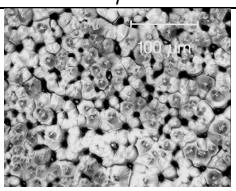
24	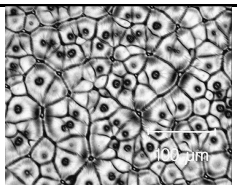	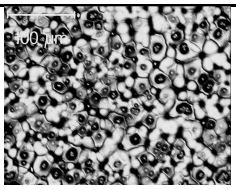
35.5	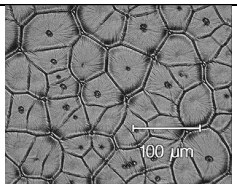	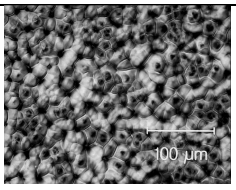
96.5	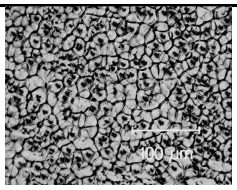	

The results of fractal analysis is presented in Fig. 7 and Fig. 8. We can observe (in chart D_0 *versus* time), that "mountainous" of surface smooth when gold goes inside (in both cases of thickness) and thus D_0 drops down. The "mountainous" of surface can also be described as levels on the map, and analysed using lacunarity. From results of lacunarity calculation, we see, that the value depends on thickness of the membrane only (Fig. 9 and Table IV). This is probably due to the fact, that a thick membrane (which is more rigid than thin one) cannot have big displacements on its surface, and

thus has them smaller, but more in quantity, instead. In this circumstances, the gold particles have more gaps to get into.

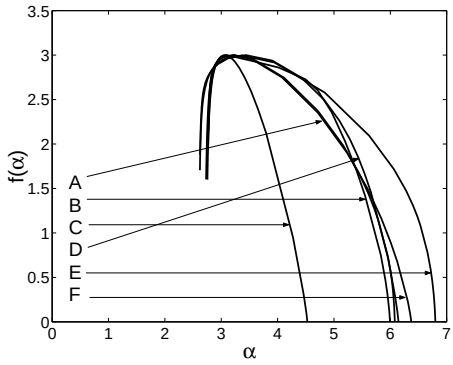

Fig. 7. Generalized fractal dimension presented as $f(\alpha)$ spectrum for morphology of polymer surfaces during gold dispersion from Table III and IV. Wide plots denote high range of mass distribution, the maximum of a plot corresponds to fractal dimension, while zeros of $f(\alpha)$ indicate, that minimum or maximum value of mass appeared only once.

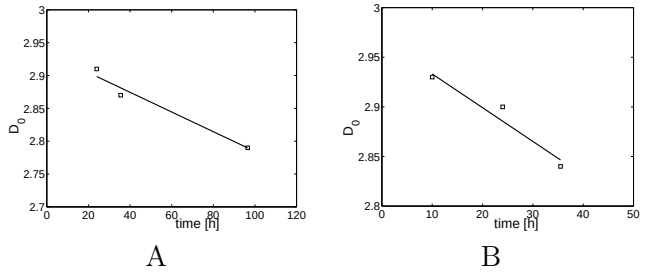

Fig. 8. Changing in structure of polymer surface during gold dispersion. Fractal dimension D_0 *versus* time for membranes of two thickness: A. 2μm and B. 3.5μm.

In the previous paper ([13]) addressed to staining in cancer cells, fractal analyses had been used to analyse differences in secretory membrane activities of two rat prostate cancer cell lines (Mat-LyLu and AT-2) of strong and weak metastatic potential, respectively. Each cell's endocytic activity had been determined by horseradish peroxidase uptake. Digital imaging showed that Mat-LyLu cells took up more label (*i.e.* were more endocytic) than AT-2 cells. The patterns of staining had been evaluated by multifractal analyses: Generalized fractal dimension (D_q), as well as Partitioned Iterated Function System — Semifractal (PIFS-SF) analysis [14]. These approaches had revealed that under control conditions, all multifractal pa-

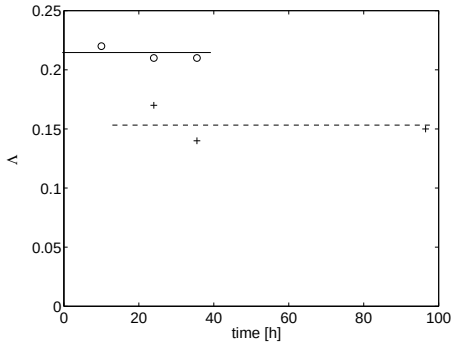

Fig. 9. Changes in structure and morphology of surface of polymer membrane (measured by lacunarity) during gold dispersion for two membrane thicknesses. The symbols in the figure are: o, —— – for 3.5μm, +, - - - – for 2μm.

TABLE IV

Structure and morphology of polymer surface during gold dispersion.

Name	Thickness [μm]	Time of dispersion [h]	Λ	D_0
A	3.50	10.0	0.22 ± 0.01	2.93 ± 0.01
B	2.00	24.0	0.17 ± 0.01	2.91 ± 0.01
C	3.50	24.0	0.21 ± 0.01	2.90 ± 0.01
D	2.00	35.5	0.14 ± 0.01	2.87 ± 0.01
E	3.50	35.5	0.21 ± 0.01	2.84 ± 0.01
F	2.00	96.5	0.15 ± 0.01	2.79 ± 0.01

rameters and PIFS-SF codes had values greater for Mat-LyLu than AT-2 cells. This would agree generally with the endocytic/vesicular activity of the strongly metastatic Mat-LyLu cells being more developed than the corresponding weakly metastatic AT-2 cells. All the parameters under study had presented sensitivity to tetrodotoxin (TTX) pre-treatment of the cells, which blocked voltage-gated Na^{2+} channels (VGSCs). In the preset work we would like to check if lacunarity can enhance this analysis. Previously used tools: D_q and PIFS-SF are invariant to flipping, mirroring, rotating (by 90°, 180° and 270°) (lacunarity Λ also) and shuffling of a given image. Lacunarity is more sensitive however for finding quality difference between pattern of staining in cell line then any of so far used techniques.

For cases, which we analyze in this paper we obtain: ($\Lambda = 0.84 \pm 0.13$ for AT-2 in control condition, $\Lambda = 0.67 \pm 0.15$ Mat-LyLu in control condition, $\Lambda = 0.68 \pm 0.20$ for AT-2 with TTX, $\Lambda = 0.77 \pm 0.25$ for Mat-LyLu with TTX). We can observe, that the range of various types of staining in the same cell line, held in the same conditions, is very large (Fig. 10 and Table V), *i.e.* the variances of different cell lines overlap. This shows, that lacunarity, as calculated by the NIH ImageJ program does not properly resolve between those cell lines. The large uncertainty in lacunarity value Λ stems from application of two averaging procedures, *(i)* with regard to gliding box size and *(ii)* number of cells.

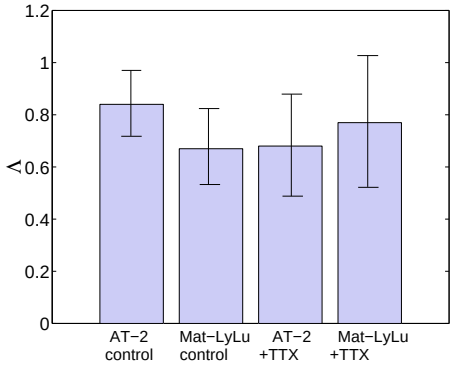

Fig. 10. Average value of lacunarity for two type of cancer cell lines in two different conditions (control condition and after blocked voltage-gated Na^{2+} channels by using TTX.)

TABLE V

Endocytotic measure E, fractal dimension D_0, range of self-similarity $\Delta D = D_{-\infty} - D_{\infty}$, number of PIFS-SF codes $N_{\mathrm{PIFS-SF}}$ and lacunarity Λ for two type of cancer cell lines in two different conditions (control condition and after blocked voltage-gated Na^{2+} channels by using TTX.)

	AT-2 control	Mat-LyLu control	AT-2 with TTX	Mat-LyLu with TTX
$E[\%]$	3.50 ± 0.20	7.90 ± 0.20	3.50 ± 0.20	3.40 ± 0.03
D_0	1.43 ± 0.05	1.68 ± 0.05	1.41 ± 0.05	1.45 ± 0.05
ΔD	1.62 ± 0.05	1.44 ± 0.05	1.60 ± 0.05	0.78 ± 0.05
$N_{\mathrm{PIFS-SF}}$	81 ± 20	153 ± 25	76 ± 20	51 ± 20
Λ	0.84 ± 0.13	0.67 ± 0.15	0.68 ± 0.20	0.77 ± 0.25

To deal with this case, we have developed our own program for lacunarity calculation. In this program we add possibility to calculate lacunarities at arbitrary gliding box sizes (the best gliding box size for cancer cells was 15 pixels for the zoom of inspected microscope), and the possibility to calculate lacunarities over irregular shapes. Also, moments were calculated in two different ways: for one feature we do this as specified by definition, and for second omitting the white peak of histogram (this corresponds to calculation of lacunarity only in places where there are some holes, so it helps to focus attention on the hole properties rather than on the density of image). In this way, we end up with two features, which are sufficient to discriminate AT-2 and Mat-LyLu cancer cells (Fig. 11).

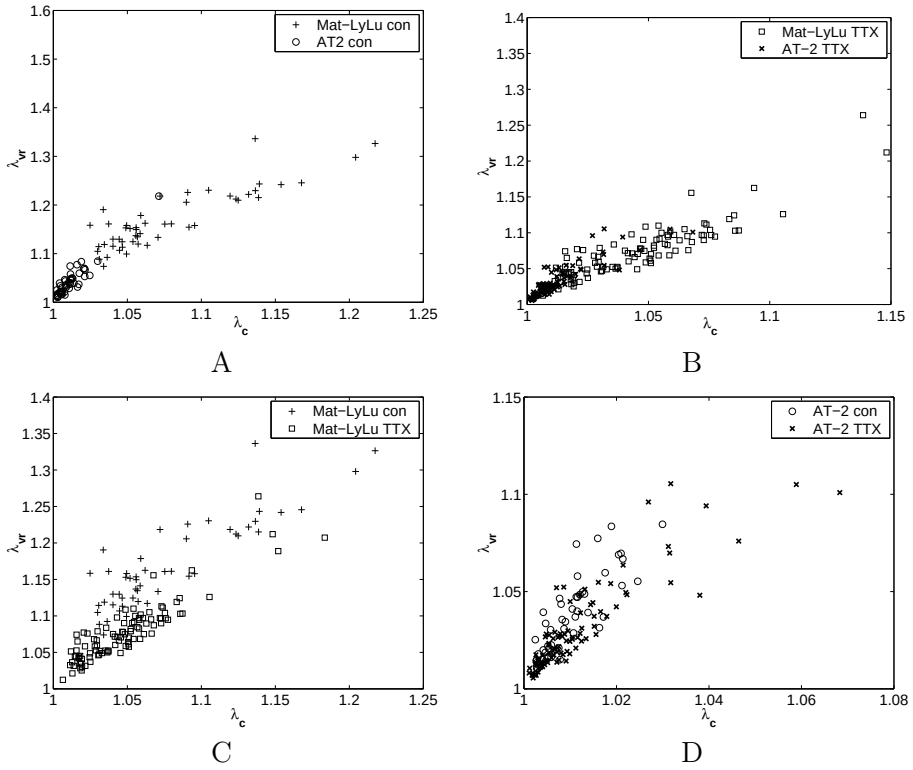

Fig. 11. Lacunarity of vacuole region *versus* lacunarity of cell for four cases. A — Mat-LyLu and AT-2 in control conditions, B — Mat-LyLu and AT-2 in TTX, C — Mat-LyLu in control conditions and Mat-LyLu in TTX, D — AT-2 in control conditions and AT2 in TTX.

5. Concluding remarks

The geometry or structure of sets can be characterized by generalized fractal dimension that can be viewed also as a measure of their irregularity. But, simple visual inspection shows that there are cases in which several sets with the same fractal (or generalized) dimension show differences in texture. In such cases the lacunarity appears to be a right tool to get rid of this discrepancy, but its use needs attention and care (especially the size of gliding box, and region of analysis is of critical importance).

We have investigated the nature of negative correlation of Λ to D_0 through analysis of the slope and intercept of equation, in which Λ and D_0 is determined by image generation rule. There is a hope that uniqueness of the image generation rule implies the linear correlation between Λ and D_0.

In case of the gold dispersion, based on SEM images, we observe surface morphology. D_q and $f(\alpha)$ show that regularity (self-similarity) of surface morphology depends on time of dispersion. After 96.5 h we have the structure of the biggest regularity. There is a linear correlation between the morphology (in the sense of D_0, which equals fractal dimension d_F) and time of gold dispersion. The obtained result shows that the surface becomes more regular due to the gold dispersion inside the polycarbone membrane. We can also observe that lacunarity depends on membrane thickness, which is not the case for the fractal dimension.

Pattern of staining, which measures endocytic membrane activity E, depends on the kind of the cells (normal cells, weakly and strongly metastatic cells) and on experimental conditions (*e.g.* tetrodotoxin sensitivity). Endocytic membrane activity E in control conditions is different for each cell line. Quantity of uptaken HRP is bigger for strongly metastatic cells Mat-LyLu. The fractal analysis (D_0) and PIFS-SF codes have confirmed this result. After blocking the activity of Na^{2+} channel (by using tetrodotoxin TTX) in Mat-LyLu cells, the decrease in number of staining is observed. TTX had no effect on HRP uptake in the AT-2 cells. Self-similarity of strongly metastatic cells after blocking Na^{2+} channel is two times higher than in control conditions. We don't observe this effect for weakly metastatic cell line. Lacunarity appeared here to be a measure, which can distinguish between AT-2 and Mat-LyLu cell lines; in control, as well as in TTX conditions. But to make it work, we had to implement our own program, with additional features, comparing to the NIH program.

Concluding, we can say that lacunarity can be used as a supplementary tool for quantitative analysis of texture of self-similar patterns of a very different nature.

We are very grateful to Prof. M.B.A. Djamgoz and Dr M. Mycielska for helpful discussions and for providing us with the experimental data of cancer cells. We also greatly acknowledge the support of the Silesian University of Technology grant BK200/RCH4/03.

REFERENCES

[1] B.B. Mandelbrot, *The Fractal Geometry of Nature*, W.H. Freeman, New York 1983.

[2] Z.J. Grzywna, M. Krasowska, L. Ostrowski, J. Stolarczyk, *Acta Phys. Pol. B* **32**, 1561 (2001).

[3] Z.J. Grzywna, M. Krasowska, *Inz. Mat.* **4**, 369 (2001).

[4] G.S. Armatas, K.M. Kolonia, P.J. Pomonis, *Langmuir* **18**, 10421 (2002).

[5] A.J. Einstein, H. Wu, J. Gil, *Phys. Rev. Lett.* **80**, 397 (1998).

[6] C. Allain, M. Cloitre, *Phys. Rev.* **A44**, 3552 (1991).

[7] R.E. Plotnick, R.H. Gardner, R.V. O'Neill, *Landscape Ecology* **3**, 201 (1993).

[8] R.E. Plotnick, R.H. Gardner, W.W. Hargrove, K. Prestegaard, M. Perlmutter, *Phys. Rev.* **E77**, 5461 (1996).

[9] T.G. Smith, G.D. Lange, W.B. Marks, *J. Neurosci. Meth.* **69**, 123 (1996).

[10] B.H. Kaye, *A Random Walk Through Fractal Dimensions*, VCH Publisher, New York 1989.

[11] R. Stoop, *Acta Phys. Pol. B* **23**, 323 (1992).

[12] J. Stolarczyk, K. Koziol, Z.J. Grzywna, *Polymer* **45**, 1525 (2004).

[13] M. Krasowska, Z.J. Grzywna, M. Mycielska, M.B.A. Djamgoz, *Eur. J. Biophys.* **33** (2004).

[14] Z.J. Grzywna, J. Stolarczyk, *Chaos, Solitons and Fractals* **13**, 897 (2002).